



ELSEVIER

Journal of Alloys and Compounds 228 (1995) 132–136

Journal of
ALLOYS
AND COMPOUNDS

Crystallographic and magnetic properties of ternary nitrides of the type $\text{RCo}_{10}\text{Mo}_2\text{N}_x$

T. Zhao, Z.G. Zhao, F.R. de Boer, K.H.J. Buschow

Van der Waals-Zeeman Laboratory, University of Amsterdam, Valckenierstraat 65, 1018 XE Amsterdam, Netherlands

Received 24 March 1995

Abstract

The magnetic and crystallographic properties of rare earth-based interstitial nitrides of the type $\text{RCo}_{10}\text{Mo}_2\text{N}_x$ ($\text{R} = \text{Ce}, \text{Pr}, \text{Nd}, \text{Sm}, \text{Gd}, \text{Tb}, \text{Dy}, \text{Ho}, \text{Er}$ and Y) were investigated by means of X-ray diffraction, high-field measurements and a.c. susceptibility measurements. From X-ray diffraction it was derived that the interstitial hole filling remains substantially below one nitrogen atom per formula unit $\text{RCo}_{10}\text{Mo}_2\text{N}_x$. We determined the easy magnetization direction in these compounds and found that the Co sublattice anisotropy favours an easy moment direction along the c -axis. The rare earth sublattice anisotropy is governed by a positive value of the second-order crystal field parameter. The large uniaxial anisotropy and the atomic disorder favour the occurrence of a thermally activated intrinsic coercivity in some of the nitrides.

Keywords: Ternary nitrides; Crystallographic properties; Magnetic properties; Intermetallic compounds

1. Introduction

Many novel Fe-rich rare earth-based permanent magnetic materials have comparatively low Curie temperatures and hence require nitrogenation for Curie temperature enhancement. Well-known examples are R_2Fe_{17} , RFe_{11}Ti and $\text{RFe}_{10}\text{Mo}_2$ [1–3]. The filling of interstitial holes by nitrogen atoms has, however, in most of these Fe-based compounds also a strong influence on the saturation magnetization and the magnetocrystalline anisotropy. Little experimental information is available on the property changes induced by charging Co-based compounds with nitrogen. In order to study the effects of interstitial hole filling in such materials we have investigated the crystallographic and magnetic properties of the compounds $\text{RCo}_{10}\text{Mo}_2\text{N}_x$, which were synthesized for the first time.

2. Experimental

The compounds of the type $\text{RCo}_{10}\text{Mo}_2$ were prepared by arc melting stoichiometric mixtures of the metallic constituents of at least 99.9% purity. After arc

melting, the polycrystalline specimens were wrapped in tantalum foil, sealed into evacuated quartz tubes and annealed at 1000°C for 4 weeks. The samples were quickly cooled to room temperature after annealing by breaking the quartz tubes under water. Subsequently, the samples were investigated by X-ray powder diffraction and found to be approximately single phase. The X-ray patterns were indexed on the basis of the ThMn_{12} type of structure.

The annealed materials were ground to fine powders with diameter less than 40 μm to provide enough active surface for the nitrogenation. The nitrogenation was carried out in a resistance furnace with a floating nitrogen atmosphere of purity better than 99.99%. The powder was kept in a quartz container inside the quartz tube. Before nitrogenation, at room temperature, the quartz tube with the samples inside was washed by the floating nitrogen gas for about 1 h to remove the air. The nitrides were formed after a heat treatment at about 600°C for nearly 15 h. Although the nitride already begins to form at lower temperatures and shorter reaction times, we found that longer reaction times and higher reaction temperatures are preferable if a single nitride phase is required. As will be discussed below, the drawback of this procedure is

the occurrence of a substantial portion of decomposition products, like RN and Co(Mo), accompanying the nitride phase.

The magnetic isotherms of the $\text{RCo}_{12-x}\text{Ti}_x$ compounds were measured in the High-field Installation at the University of Amsterdam [4]. The measurements were performed on free powders and incidentally on magnetically aligned powders. The isotherms of the latter samples were studied with the measuring fields applied parallel and perpendicular to the alignment field. Measurements of the temperature dependence of the a.c. susceptibility were performed to study the presence of spin reorientations between room temperature and 4.2 K.

3. Experimental results and discussion

3.1. X-ray diffraction

The structure and purity of the nitrides were checked by X-ray diffraction. The diffraction patterns of the nitrides are similar to those of the parent compounds, albeit all reflection peaks have shifted to lower angle positions upon nitrogenation. The diffraction peaks have remained comparatively sharp, indicating that only a single nitride phase has formed. No peaks corresponding to second phase are found. For instance, elemental Co which is usually present in Co-rich R-Co samples, has not been found in the X-ray diffraction patterns of all nitrides investigated (see Fig. 1, for example). In order to determine the lattice constants accurately, silicon has been used as a calibration standard. The lattice parameters obtained are listed in Table 1. One can see from this table that the lattice expansion is 1.25–2.03%, which is just half the value found in the corresponding $\text{RFe}_{10}\text{Mo}_2\text{N}_x$ compounds, where $x = 1$ [1,2]. However, by compar-

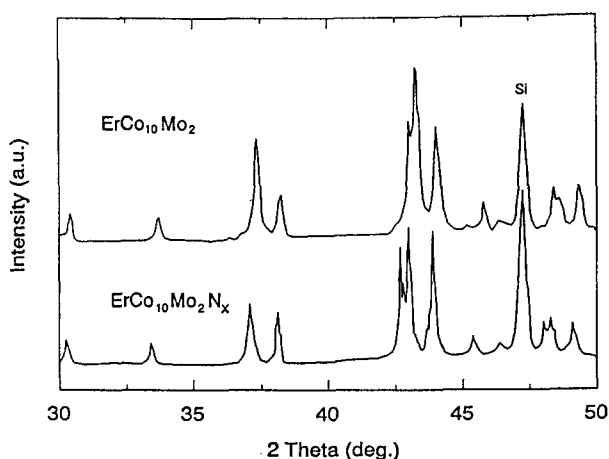


Fig. 1. X-ray patterns of $\text{ErCo}_{10}\text{Mo}_2$ and $\text{RCo}_{10}\text{Mo}_2\text{N}_x$.

Table 1
Structural parameters of $\text{RCo}_{10}\text{Mo}_2$ and $\text{RCo}_{10}\text{Mo}_2\text{N}_x$

Compound	a (Å)	c (Å)	V (Å ³)	c/a	$\Delta V/V$
$\text{YCo}_{10}\text{Mo}_2$	8.4164	4.7144	333.95	0.560	
$\text{YCo}_{10}\text{Mo}_2\text{N}_x$	8.4787	4.7212	339.40	0.557	1.63%
$\text{CeCo}_{10}\text{Mo}_2$	8.4075	4.7143	333.24	0.561	
$\text{CeCo}_{10}\text{Mo}_2\text{N}_x$	8.4737	4.7352	340.00	0.559	2.03%
$\text{PrCo}_{10}\text{Mo}_2$	8.4632	4.7263	338.45	0.560	
$\text{PrCo}_{10}\text{Mo}_2\text{N}_x$	8.5073	4.7537	344.04	0.559	1.65%
$\text{NdCo}_{10}\text{Mo}_2$	8.4522	4.7212	337.28	0.559	
$\text{NdCo}_{10}\text{Mo}_2\text{N}_x$	8.5140	4.7518	344.45	0.558	2.13%
$\text{SmCo}_{10}\text{Mo}_2$	8.4499	4.7348	338.66	0.560	
$\text{SmCo}_{10}\text{Mo}_2\text{N}_x$	8.5114	4.7569	344.61	0.559	1.76%
$\text{GdCo}_{10}\text{Mo}_2$	8.4251	4.7136	334.59	0.559	
$\text{GdCo}_{10}\text{Mo}_2\text{N}_x$	8.4658	4.7418	339.85	0.560	1.57%
$\text{TbCo}_{10}\text{Mo}_2$	8.4051	4.7042	332.38	0.560	
$\text{TbCo}_{10}\text{Mo}_2\text{N}_x$	8.4654	4.7266	338.72	0.558	1.91%
$\text{DyCo}_{10}\text{Mo}_2$	8.4079	4.7105	333.00	0.560	
$\text{DyCo}_{10}\text{Mo}_2\text{N}_x$	8.4792	4.7284	339.75	0.557	2.03%
$\text{HoCo}_{10}\text{Mo}_2$	8.4056	4.7071	332.58	0.560	
$\text{HoCo}_{10}\text{Mo}_2\text{N}_x$	8.4556	4.7099	336.75	0.557	1.25%
$\text{ErCo}_{10}\text{Mo}_2$	8.4059	4.7087	332.72	0.560	
$\text{ErCo}_{10}\text{Mo}_2\text{N}_x$	8.4637	4.7219	338.25	0.558	1.66%

ing the masses of the samples before and after nitrogenation we found that the nitrogen concentration in the $\text{RCo}_{10}\text{Mo}_2\text{N}_x$ samples corresponds roughly to $x = 1$ also. This can be taken as an indication that the nitrogen is present in the samples in a different form. It means that considerable decomposition of the metastable $\text{RCo}_{10}\text{Mo}_2\text{N}_x$ nitrides into RN and Co(Mo) had taken place during the high-temperature treatment. The phase separation into RN and Co(Mo) requires long-range diffusion of the metal atoms. This process is known to be incomplete during the comparatively short nitrogenation times and to lead to either amorphous or microcrystalline products which escape detection by standard X-ray diffraction.

It can be seen from Table 1 that the expansion caused by nitrogenation is anisotropic. The expansion is mainly along the (a,b) plane and the c/a ratio decreases upon nitrogenation. These results are similar to those observed in $\text{RFe}_{10}\text{Mo}_2\text{N}_x$ and imply that nitrogen occupies the 2b sites in the ThMn_{12} -type structure [1].

From the X-ray diffraction experiments made on magnetically aligned powders, it was derived that the easy magnetic direction in the $\text{RCo}_{10}\text{Mo}_2\text{N}_x$ compounds is parallel to the c -axis at room temperature.

3.2. Magnetic measurements

In order to investigate the presence of spin reorientation transitions between 4.2 K and room temperature, several compounds were investigated by means of a.c. susceptibility measurements. A peak corresponding to a spin reorientation was found only in $\text{ErCo}_{10}\text{Mo}_2\text{N}$. The peak corresponds to a spin

reorientation from $M \perp c$ at low temperature to $M \parallel c$ at high temperature, as has also been observed in the uncharged compound [5]. This result shows that the second-order crystal field parameter A_2^0 has retained its positive value upon nitrogeneration. The spin reorientation temperature is 10 K lower than in $\text{ErCo}_{10}\text{Mo}_2$. It is difficult to decide whether this is due to a relative decrease of the easy plane anisotropy of the rare earth sublattice or to a relative increase of the easy axis anisotropy of the Co sublattice upon nitrogeneration.

The compounds $\text{NdCo}_{10}\text{Mo}_2\text{N}_x$ and $\text{PrCo}_{10}\text{Mo}_2\text{N}_x$ were found to display a strong intrinsic coercivity at low temperatures. Results for the latter compound are shown in Fig. 2(a). These were obtained on a powder sample magnetically aligned at room temperature and measured at low temperatures with the field applied parallel to the alignment direction.

The wasp-tailed hysteresis loops obtained at various

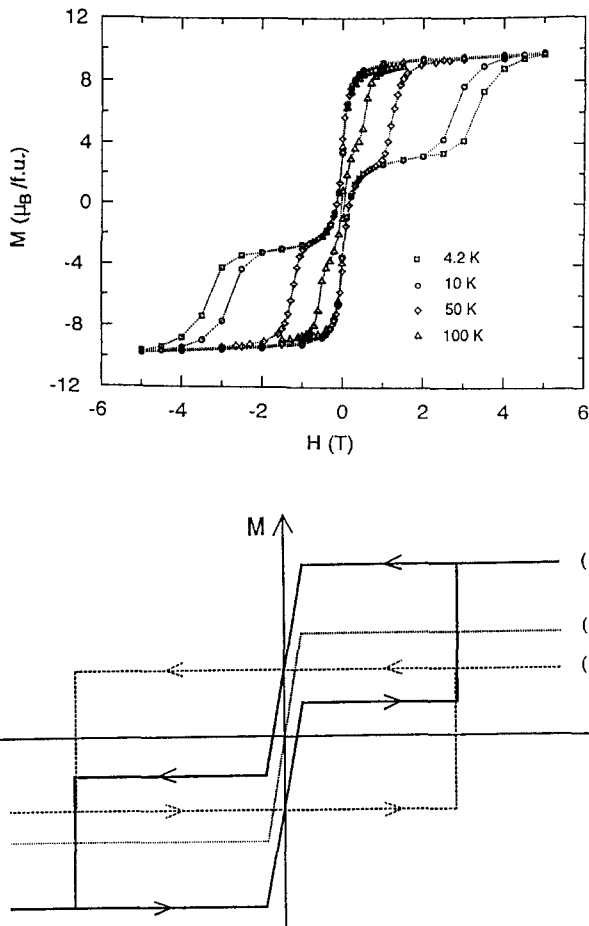


Fig. 2. (a) Hysteresis loops of $\text{PrCo}_{10}\text{Mo}_2\text{N}_x$ at different temperatures measured on magnetically aligned powders with the external field parallel to the alignment direction. (b) Schematic representation of the decomposition of the wasp-tailed hysteresis loops into a component without coercivity (dotted curve, b) and a component with large coercivity (broken curve, a). The total loop is obtained by adding the contributions of both components (full curve, c).

temperatures can be decomposed into two parts. This decomposition is schematically illustrated in Fig. 2(b), where one recognizes the contribution of the main part, having almost no coercivity, and the contribution of the minority part, having a large coercivity. The temperature dependence of the coercivity of the latter part is shown in Fig. 3. It can be inferred from the results shown in Fig. 3 that the coercivity depends exponentially on temperature.

The occurrence of an intrinsic coercive force and its exponential temperature dependence is commonly attributed to thermally activated wall motion caused by potential energy barriers that keep the walls in stable positions. The walls have to be fairly narrow, requiring a high anisotropy energy relative to the exchange energy. Most of the systems in which thermally activated wall motion has been observed display some type of atomic disorder (amorphous alloys or pseudobinary compounds [6,7]) giving rise to concentration fluctuations and hence to local fluctuations of the anisotropy field that can serve as wall-pinning centres.

In the presently investigated materials, one can envisage such pinning centres as arising through fluctuations of the nitrogen concentration. Here, one has to bear in mind that complete filling of the interstitial 2b site would correspond to $x = 1$ in $\text{PrCo}_{10}\text{Mo}_2\text{N}_x$. From X-ray diffraction we derived that x is far below this limit, meaning that there will be a distribution of Pr atoms having 0, 1 or 2 nearest-neighbour N atoms. It has been shown elsewhere that full N atom occupation of the two interstitial sites around the rare earth position in these ThMn_{12} -type compounds leads to a

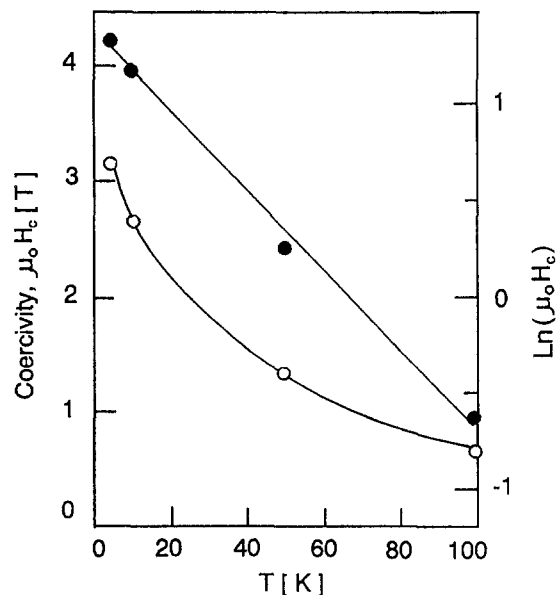


Fig. 3. Temperature dependence of the coercivity of $\text{PrCo}_{10}\text{Mo}_2\text{N}_x$ (open circles, left scale) and temperature dependence of the logarithm of the coercivity (filled circles, right scale).

strong anisotropy enhancement [6] which identifies the pinning centres as regions where the N concentration is high in $\text{PrCo}_{10}\text{Mo}_2\text{N}_x$. Our experimental data do not allow us to decide whether the fraction of the material that does not display an intrinsic coercivity is to be attributed to regions in $\text{PrCo}_{10}\text{Mo}_2\text{N}_x$ where the N concentration is low or to the presence of the decomposition products.

Free-powder magnetization measurements in fields up to 21 T at 4.2 K have been performed on all the nitrides. Examples of magnetic isotherms obtained in this way are shown in Fig. 4. All these measurements were made with decreasing field strength so that the influence of the hysteretic phenomena described above is absent here. Values of the saturation magnetization $M(0)$, obtained by extrapolation of the low-field parts of the isotherms to $B = 0$ are listed in Table 2.

We have taken the saturation moments obtained from the $\text{RCo}_{10}\text{Mo}_2\text{N}_x$ compounds and used these values in conjunction with the free-ion moment M_R of the R sublattice to obtain an estimate (M_{Co}) of the Co sublattice moment. As is customary, we have assumed parallel (antiparallel) R and Co moment coupling for

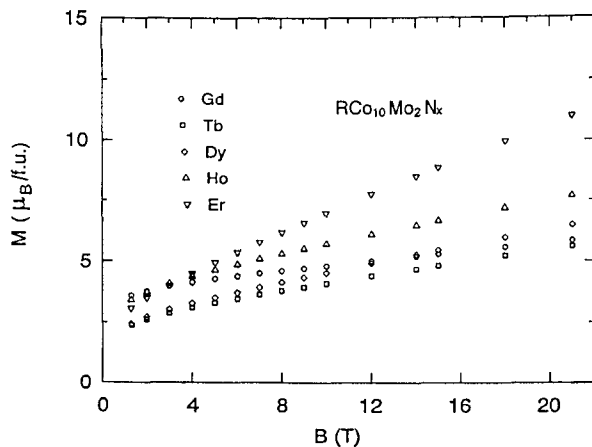


Fig. 4. Magnetic isotherms at 4.2 K of $\text{RCo}_{10}\text{Mo}_2\text{N}_x$ compounds (R = Gd, Tb, Dy, Ho and Er) measured on powder particles that are free to rotate in the sample holder.

Table 2
Magnetic properties of $\text{RCo}_{10}\text{Mo}_2\text{N}_x$ compounds

Compound	M_R (μ_B /f.u.)	$M(0)$ (μ_B /f.u.)	M_{Co} (μ_B /f.u.)	n_{RT} (T^2J^{-1} f.u.)	J_{RT}/k (K)
$\text{YCo}_{10}\text{Mo}_2\text{N}_x$	0	8.36	8.36	—	—
$\text{CeCo}_{10}\text{Mo}_2\text{N}_x$	0	8.48	8.48	—	—
$\text{PrCo}_{10}\text{Mo}_2\text{N}_x$	3.20	10.46	7.26	—	—
$\text{NdCo}_{10}\text{Mo}_2\text{N}_x$	3.27	11.06	7.79	—	—
$\text{SmCo}_{10}\text{Mo}_2\text{N}_x$	0.71	8.91	8.20	—	—
$\text{GdCo}_{10}\text{Mo}_2\text{N}_x$	7.00	3.94	10.94	10.0	8.1
$\text{TbCo}_{10}\text{Mo}_2\text{N}_x$	9.00	2.78	11.78	7.9	8.8
$\text{DyCo}_{10}\text{Mo}_2\text{N}_x$	10.00	2.89	12.89	6.0	9.0
$\text{HoCo}_{10}\text{Mo}_2\text{N}_x$	10.00	3.98	13.98	5.2	9.1
$\text{ErCo}_{10}\text{Mo}_2\text{N}_x$	9.00	3.87	13.87	2.8	6.3

the light (heavy) R elements. Comparison of this set of values with the value of M_{Co} for $\text{YCo}_{10}\text{Mo}_2\text{N}_x$ shows that the M_{Co} values obtained for the compounds in which R is a light magnetic rare earth element are lower, and those for the heavy rare earths are higher than the former value. We mentioned already that a considerable amount of decomposition of the $\text{RCo}_{10}\text{Mo}_2\text{N}_x$ compounds into RN and Co(Mo) has occurred during the high-temperature reaction. Both decomposition products are ferromagnetic at 4.2 K [8]. Because of the amorphous or microcrystalline character of the decomposition products, a small moment loss can be envisaged for the compounds with light rare earth elements. By contrast, a strong moment gain is expected for the compounds of the heavy rare earths, owing to the antiparallel coupling of the R and Co moments in the undecomposed material.

Finally, we have used the linear high-field part of the isotherms of the $\text{RCo}_{10}\text{Mo}_2\text{N}_x$ compounds with R = Gd, Tb, Dy, Ho and Er to determine the magnetic coupling strengths between the rare earth sublattice moment and the transition metal (T) sublattice moment. As has been outlined in detail elsewhere [9,10], one may use the slope of the linear high-field parts:

$$n_{\text{RT}} = (dB/dM)^{-1} \quad (1)$$

to obtain experimental values of the intersublattice coupling constant J_{RT} by means of the molecular field expression

$$n_{\text{RT}} = \frac{J_{\text{RT}}Z_{\text{RT}}(g_{\text{R}} - 1)}{N_{\text{T}}\mu_{\text{B}}^2g_{\text{R}}} \quad (2)$$

where $Z_{\text{RT}} = 20$ is the number of nearest transition metal (T) atoms to an R atom in RT_{12} and where $N_{\text{T}} = 12$ is the number of T atoms per formula unit. Values of n_{RT} and J_{RT} obtained from the experimental data by means of Eqs. (1) and (2) have been included in Table 1. The values listed for J_{RT} are very close to the values derived earlier for compounds of the series $\text{RCo}_{10}\text{Mo}_2$ [5,10]. Apparently, nitrogenation does not

much affect the magnetic exchange coupling between the R and the Co sublattice.

4. Concluding remarks

We have investigated the changes in magnetic and crystallographic properties upon nitrogenation of ThMn₁₂-type RCo₁₀Mo₂N_x compounds. From X-ray diffraction we derived that the lattice expands anisotropically upon nitrogenation. As in the corresponding Fe-based compounds, the nitrogen atoms prefer to occupy the interstitial 2b sites, but fill approximately only half of the interstitial holes. During the nitrogenation, considerable decomposition of the nitrides has taken place, which made it impossible to determine whether nitrogenation has led to a change of the Co moment. The large magnetic anisotropies in NdCo₁₀Mo₂N_x and PrCo₁₀Mo₂N_x in conjunction with the atomic disorder give rise to an intrinsic coercivity at low temperatures. From the temperature dependence of the coercivity it was derived that domain wall motion is a thermally activated process. The inter-sublattice exchange interaction was found to remain almost unchanged upon nitrogenation.

References

- [1] H. Sun, Y. Morii, H. Fujii, M. Akayama and S. Funahashi, *Phys. Rev.*
- [2] H. Sun and H. Fujii, in K.H.J. Buschow (ed.), *Magnetic Materials*, Vol. 9, Elsevier Science Publishers, Amsterdam, 1995.
- [3] K.H.J. Buschow, *Rep. Progr. Phys.*, 54 (1991) 1123.
- [4] R. Gersdorf, F.R. de Boer, J. Wolfrat, F.A. Muller and L.W. Roeland, in M. Date (ed.), *High-field Magnetism*, North-Holland, Amsterdam, 1983, p. 277.
- [5] D.C. Zeng, N. Tang, T. Zhao, Z.G. Zhao, K.H.J. Buschow and F.R. de Boer, *J. Appl. Phys.*, 76 (1994) 6837.
- [6] D.P. Middleton, F.M. Mulder, R.C. Thiel and K.H.J. Buschow, *J. Magn. Magn. Mater.*, 146 (1995) 123.
- [7] K.H.J. Buschow, in K.A. Gschneidner and L. Eyring (eds.), *Handbook of the Physics and Chemistry of Rare Earths*, Vol. 7, North-Holland, Amsterdam, 1984, p. 265; K.H.J. Buschow, *Rep. Progr. Phys.*, 40 (1977) 1123.
- [8] J.A. Gibson and G. Harvey, *Tech. Report AFML-TR-65-430*, Batelle Memorial Institute.
- [9] R. Verhoef, P.H. Quang, J.J.M. Franse and R.J. Radwanski, *J. Magn. Magn. Mater.*, 74 (1988) 43.
- [10] J.P. Liu, F.R. de Boer, P.F. de Châtel, R. Coehoorn and K.H.J. Buschow, *J. Magn. Magn. Mater.*, 132 (1994) 159.